EUROPEAN ORGANIZATION FOR NUCLEAR RESEARCH

CERN-EP/86-57
May 15th, 1986

ANTIPROTON-PROTON CROSS SECTIONS AT 200 AND 900 GEV C.M.ENERGY

UA5 Collaboration

Bonn[1], Brussels[2], Cambridge[3], CERN[4] and Stockholm[5]

G.J.Alner[3*], R.E.Ansorge[3], B.Åsman[5], C.N.Booth[3+], L.Burow[1], P.Carlson[5], C.DeClercq[2], R.S.DeWolf[3], A. Drees[1], B.Eckart[1], G.Ekspong[5], I.Evangelou[4$], A.Eyring[1], J.-P.Fabre[4], L.Fröbel[1], C.Fuglesang[5], J.Gaudaen[2‡+], C.Geich-Gimbel[1], B. Holl[1], G.von Holtey[4], R.Hospes[1], K.Jon-And[5], Th.Kokott[1], F.Lotse[5], N.Manthos[4$], R.Meinke[1], D.J.Munday[3], J.E.V.Ovens[3], W.Pelzer[1], J.Reidy[4×], J.G.Rushbrooke[3], H.Schmickler[1], F.Triantis[4$], L.Van hamme[2], Ch.Walck[5], C.P.Ward[3], D.R.Ward[3], C.J.S.Webber[3], T.O.White[3], G.Wilquet[2] and N.Yamdagni[5].

1 Physikalisches Institut der Universität Bonn, Germany
2 Inter-University Institute for High Energies (ULB-VUB), Brussels, Belgium
3 Cavendish Laboratory, Department of Physics, Cambridge University,UK
4 CERN, Geneva, Switzerland
5 Institute of Physics, University of Stockholm, Sweden

ABSTRACT

Data on antiproton-proton cross sections at the c.m. energies 200 and 900 GeV are presented. The data were obtained at the CERN antiproton-proton Collider operated in a new pulsed mode in which the same beams were accelerated and decelerated between beam energies of 450 and 100 GeV. The properties of the machine determine the ratio of the luminosities at the two energies to about 1% and thus an accurate measurement of the ratio R of the inelastic cross sections could be made. We find R ($= \sigma^{900}/\sigma^{200}$) = 1.20±0.01±0.02, where the first error is statistical and the second systematic. Interpolating existing data to estimate σ_{inel}(200 GeV) this measurement of R leads to σ_{inel}(900 GeV) = 50.3±0.4±1.0 mb. Using an extrapolated value of σ_{el}/σ_{tot} we estimate the total cross section at 900 GeV to be 65.3±0.7±1.5 mb. Both the inelastic and total cross sections are compatible with a $\ell n^2 s$ dependence. Comparisons are made with different fits to the total cross section energy dependence.

* Member of Rutherford Appleton Laboratory, Chilton, Didcot, UK.
‡ Also at the Unversitaire Instellingen Antwerpen, Antwerp, Belgium.
$ Also at the University of Ioannina, Greece.
+ Now at CERN.
× Visiting scientist from University of Mississipi.

(Submitted to Zeitschrift für Physik C, Particles and Fields)

1. INTRODUCTION

The total cross section σ_{tot} for pp and $\bar{p}p$ scattering has been shown to rise over the energy range of the ISR (c.m. energy $\sqrt{s}$ = 30-62 GeV) [1-3] and, more recently, has been shown to follow an approximate $\ell n^2 s$ dependence up to $\sqrt{s}$ = 546 GeV at the CERN antiproton-proton Collider [4]. This rate of growth is the maximum compatible with the Froissart bound [5], although the predicted coefficient of the $\ell n^2 s$ term [6] (π/m_π^2) appears to be much greater than the measured value. In an impact parameter view [7] this $\ell n^2 s$ dependence would imply that the radius of the proton is growing like $\ell n s$.

The 546 GeV measurements also show, however, that the ratio $r = \sigma_{el}/\sigma_{tot}$ has increased from a value 0.18 at the ISR to 0.22 at the Collider, thereby ruling out models which require r to be a constant, such as geometrical scaling [8], or to be constant or decrease with energy, such as Reggeon field theory with the 'critical Pomeron' [9]. Furthermore, from the impact parameter viewpoint this suggests that the opaqueness of the proton(*) has increased from about 0.36 at the ISR [7] to about 0.43 at the Collider [10,11], to be compared with the unitarity bound of 0.5 corresponding to complete absorption. Any asymptotic regime would thus seem to be far away, with the observed achievement of an early $\ell n^2 s$ dependence of σ_{tot} being evidently misleading.

Any evidence as to the likely trend of σ_{tot} at higher energy is therefore of great interest. Is the $\ell n^2 s$ dependence going to continue, or is an alternative possibility, such as σ_{tot} approaching a constant, going to occur?

The top energy of the CERN $\bar{p}p$ Collider in normal DC operation is limited mainly by the level of power dissipation that can be tolerated in the main ring magnets of the SPS. It was proposed in 1982 [12] that one could cycle the stored beams between 450 GeV and

---

(*)defined as the value of Imf(s,b) at b = 0, where f(s,b) is the scattering amplitude in terms of the impact parameter, b.

some lower energy (say 100 GeV) such that the average power consumption would not exceed that in DC Collider operation (then 270 GeV, now 315 GeV per beam). The main aim of the UA5 proposal [13] was to search for a possible threshold above $\sqrt{s}$ = 546 GeV for unusual events (Centauros, Chirons, Geminions)[14]. Furthermore an overview of hadron physics up to 900 GeV with reasonable statistics could be obtained. Following successful tests of the pulsing scheme during the summer of 1984 the dedicated physics run of the pulsed collider took place in March-April 1985.

With the UA5 detector it was possible to measure interaction rates at both 900 GeV and 200 GeV, and although the absolute values of the machine luminosity are known only to some ±10%, their ratio at 900 and 200 GeV is known to 1%, thus making possible an accurate measurement of the ratio of the cross sections at the two energies. Since the value of the cross section at 200 GeV can be found by interpolation, a value at 900 GeV can be inferred. Furthermore, the measured ratio can itself be used to investigate different asymptotic forms of the scattering amplitude, for example in terms of analytic functions [15,16].

This paper is organized as follows. The operation of the pulsed Collider and the UA5 detector is described in section 2. The experimental method is described in section 3 and the results are presented in section 4. Conclusions are given in section 5.

2. THE PULSED COLLIDER AND THE UA5 DETECTOR

2.1 The Pulsed Collider

The cycle used, depicted in figure 1, comprised a 4 s flat top at $\sqrt{s}$ = 900 GeV and an 8.4 s flat bottom at $\sqrt{s}$ = 200 GeV. The duty factor was 19% (38%) for 900 (200) GeV. New hardware and software techniques were developed [17] to reduce the machine tune (Q) variation to within ~ 0.002 at all points of the cycle. Methods were developed for measuring the tune to 0.001 every 6 ms over the cycle, the results being fed back as adjustments to the power supplies. This improved tune stability was important for the present analysis, ensuring a constant luminosity ratio between 900 GeV and 200 GeV.

Some features of the pulsed Collider performance are summarized in Table 1. Although the luminosity was much lower than during normal DC operation (mainly due to the absence of pulsed low β quadrupoles) it was entirely adequate for the physics aims of the present experiment. From the point of view of the UA5 detector, there was generally less background (beam-gas and particles lost from bunches) in the pulsed mode of operation than from Collider DC operation in 1981-82, presumably because of the improvements mentioned above.

2.2 The UA5 Detector

A schematic layout of the UA5 detector is shown in figure 2; more details can be found in ref. [18]. Two large streamer chambers, 6m x 1.25m x 0.5m, are placed above and below the 2mm thick beryllium vacuum pipe. They give an azimuthal coverage of 95% for a pseudorapidity $|\eta|<3$ ($\eta = -\ln \tan \theta/2$ where θ is the c.m. production angle) falling to zero at $|\eta| = 5$. Each chamber is viewed by three cameras and each frame contains a stereo pair of views. At each end of the chambers there is a pair of trigger hodoscopes, designated A1 and A2, covering the pseudorapidity range

$2<|\eta|<5.6$. The large solid angle covered by these hodoscopes and their good time resolution made the trigger efficient for beam-beam interactions while at the same time suppressing a good part of the beam-gas background.

Data were taken with two triggers, run in parallel, based on different combinations of the incident proton arm (A1) and the incident antiproton arm (A2). A 2-arm trigger, A1.A2, requiring at least one hit in each arm, selected mainly non single-diffractive (NSD) events. A 1-arm trigger A1.$\overline{A2}$ was used to select highly asymmetric events, for example single-diffractive (SD) events. The trigger $\overline{A1}$.A2 contained too much background from the more intense proton bunch and was not used. The relationships between the triggers and the different physical processes (elastic scattering, single diffraction and non single-diffraction) are illustrated in figure 3. The data presented in this paper are based on 59000 triggers. Of these 25000 had streamer chamber photographs which were examined.

3. EXPERIMENTAL METHOD

The rate $\dot{N}_i(t)$ for a given trigger i (1-arm or 2-arm) at any time t is related to the luminosity L(t) and the trigger cross section σ_i through

$$\dot{N}_i(t) = \sigma_i L(t) \tag{3.1}$$

Hence one can write for the ratio R of the cross sections at 900 and 200 GeV

$$R = \frac{\sigma_i^{900}}{\sigma_i^{200}} = \frac{\dot{N}_i^{900}}{\dot{N}_i^{200}} \cdot \frac{L^{200}}{L^{900}} \tag{3.2}$$

In this section we discuss first the ratio of the luminosities indicating how this ratio can be known to 1%. We then show how the trigger rates are obtained from the electronic data combined with

information from the scanning and measurement of the streamer chamber photographs. Finally we show how to relate the cross sections for physical processes (σ_{SD}, σ_{NSD}, $\sigma_{inel} = \sigma_{SD} + \sigma_{NSD}$) to the triggering cross sections for the 1-arm and 2-arm triggers (σ_1, σ_2).

3.1 Luminosity Ratio

At the Collider the luminosity may be written

$$L = f \frac{n_p n_{\bar{p}}}{A_{eff}} \tag{3.3}$$

where f(=43.4 kHz) is the revolution frequency and n_p and $n_{\bar{p}}$ are the numbers of protons and antiprotons in each bunch, the same throughout the cycle. The effective transverse area of the bunches is given by

$$A_{eff} = \frac{1}{2} \sqrt{\beta_H \beta_V (E_{pH}+E_{\bar{p}H}).(E_{pV}+E_{\bar{p}V})} \tag{3.4}$$

in terms of the machine beta-function values (β) and emittances (E), H and V denoting horizontal and vertical respectively. Approximate values of these quantities are given in Table 1. On recalling that the emittance may be written $E = \pi\varepsilon^*(\gamma^2-1)^{-1/2}$, where $\pi\varepsilon^*$ is the normalized emittance and γ the Lorentz factor of the beam, it follows that

$$\frac{L^{200}}{L^{900}} = \frac{(\beta_H \beta_V)^{1/2}_{900}}{(\beta_H \beta_V)^{1/2}_{200}} \cdot \frac{\gamma^{200}}{\gamma^{900}} \tag{3.5}$$

During the period of pulsed Collider operation, measurements [19] were made that confirmed that the ratio of the horizontal beta-functions at the two energies was unity with an upper limit to the error of ±1% and likewise for the vertical values. Analyses [20] of radio frequency settings, of the radial positions of bunches within the machine, and of extracted proton beam measurements, show that

$$\frac{\gamma^{200}}{\gamma^{900}} = 0.2238 \pm 0.0006 \qquad (3.6)$$

It follows that the luminosity ratio is 0.224 within ±1%. A study of wire scan data during the run [21] confirms this value of the luminosity ratio giving 0.22±0.03.

3.2 Trigger rates

The numbers of 1-arm and 2-arm triggers N_1 and N_2 have to be corrected for background e.g., from beam-gas interactions and scatters in the vacuum chamber of particles lost from the circulating bunches. The fractions of true beam-beam interactions were determined by scanning and measuring streamer chamber photographs. Figures 4a,b and c illustrate three classes of events: a 2-arm beam-beam interaction, a 1-arm beam-beam interaction and a background interaction. In the case of 2-arm triggers scanning was sufficient to distinguish background from beam-beam interactions as confirmed by full measurements of a sample. In the case of 1-arm triggers, obvious background events were rejected at the scanning stage, all remaining events being measured. Figure 5 shows the resulting vertex distribution along the beam axis for (a) 2-arm triggers and (b) 1-arm triggers. The widths of the distributions are the same, but in the 1-arm case there is a uniform background outside the peak, which we associate with beam-gas interactions. This background was subtracted assuming a uniform distribution under the peak. The fraction of beam-beam interactions was on average 97.2% (93.8%) for the 2-arm trigger at 900 (200) GeV. For the 1-arm trigger it was much lower, 27% (8%) at 900 (200) GeV.

During a particular fill of the Collider the trigger rates fell about an order of magnitude from the initial values of about 10 Hz and 1.5 Hz for the 2-arm and 1-arm triggers, respectively. However, corrected for background as described above, the ratios of the trigger rates at 900 and 200 GeV were found to be constant during a particular fill and also from fill to fill. This is

illustrated in figure 6 where the luminosity (a), the ratio of the corrected 2-arm trigger rates at 900 and 200 GeV (b), and the ratio of the corrected 1-arm trigger rates at 900 and 200 GeV (c), are shown.

3.3 Trigger Efficiencies

Single-diffractive events have very different triggering properties from other events. In order to determine the overall trigger efficiency we therefore divide the inelastic cross section σ_{inel} into a single-diffractive part, σ_{SD} and a non single-diffractive part σ_{NSD}:

$$\sigma_{inel} = \sigma_{SD} + \sigma_{NSD} \tag{3.7}$$

The triggering cross sections σ_1 and σ_2 for the 1-arm and 2-arm triggers, respectively, are related to σ_{SD} and σ_{NSD} by the trigger efficiencies $\varepsilon_{1,2}^{NSD,SD}$ in obvious notation:

$$\sigma_1 = \varepsilon_1^{NSD}\,\sigma_{NSD} + \varepsilon_1^{SD}\,\sigma_{SD} \tag{3.8}$$

$$\sigma_2 = \varepsilon_2^{NSD}\,\sigma_{NSD} + \varepsilon_2^{SD}\,\sigma_{SD} \tag{3.9}$$

Solving equations (3.7-3.9) gives

$$\sigma_{inel} = \chi_1\sigma_1 + \chi_2\sigma_2 \tag{3.10}$$

where $\chi_{1,2}$ are functions of $\varepsilon_{1,2}^{SD}$ and $\varepsilon_{1,2}^{NSD}$.
Combining eq. (3.10) with eq.(3.2) one has finally

$$R = \frac{\sigma_{inel}^{900}}{\sigma_{inel}^{200}} = \frac{[2\chi_1 N_1+\chi_2 N_2]^{900}}{[2\chi_1 N_1+\chi_2 N_2]^{200}} \cdot \frac{L^{200}}{L^{900}} \cdot \frac{t^{200}}{t^{900}} \tag{3.11}$$

where $N_{1,2}$ are the corrected numbers of counts obtained in a trigger active time t. The extra factor of 2 appearing in eq.(3.11) results from the use of only one of the two 1-arm trigger combinations. Note that figures 6(b) and (c) correspond to putting in turn $\chi_1 = 0$, $\chi_2 = 1$,

and $\chi_1 = 1$, $\chi_2 = 0$ in eq. (3.11).

The trigger efficiencies $\varepsilon_{1,2}^{NSD}$ for the non single-diffractive component were estimated using the UA5 cluster Monte Carlo [22], which has been tuned to reproduce observed features of particle production up to 900 GeV.

For the single diffractive component an event generator was used that incorporated an s/M^2 dependence of the invariant cross-section [23], a longitudinal phase-space decay of the diffractive system with mass M, a decay multiplicity of the system M following a ℓn M dependence and a lower cut-off in M of 1.08 GeV ($= M_p + M_\pi$). An upper limit to M was taken from $M^2/s<0.05$. The distribution of the momentum transfer squared to the recoil system, t, was taken to be $e^{-7|t|}$. The values obtained for the trigger efficiencies are given in Table 2. Correlations between systematic errors in the efficiencies cause their effect largely to cancel in the ratio of the cross-sections at 200 and 900 GeV. As a check on the validity of our event generators, we compare in figure 7 the pseudorapidity gap distribution for the 1-arm triggers with the results of our simulation. The form of the simulated distribution is sensitive to the mixture of single diffractive and non single-diffractive components, and the good agreement is a consistency check on our simulation procedures.

4. RESULTS AND DISCUSSION

Using eq. (3.11) we get the following result for the ratio of the inelastic cross sections at 900 and 200 GeV:

$$R_{inel} = \frac{\sigma_{inel}^{900}}{\sigma_{inel}^{200}} = 1.20 \pm 0.01 \pm 0.02$$

This value of R is the slope of the straight line in fig.8, which is a plot of $\dot{N}^{900} L^{200}/L^{900}$ against $\dot{N}^{200}$. The first error in R is statistical, and the second systematic. The relative contribution of the different sources of systematic errors to the error in R are given

in Table 3. The systematic errors in the determination of the interaction rates operate in the same direction at both energies. Therefore these errors tend to cancel in the ratio.

4.1 Absolute values of σ^{900}_{inel}, σ^{900}_{tot}

To obtain absolute values of the cross sections we use the recent fit to σ_{tot} by Amos et al. [3] which gives $\sigma^{200}_{tot} = 51.6 \pm 0.4$ mb. To get the inelastic cross section we need the ratio σ_{el}/σ_{tot} which has been measured at $\sqrt{s} = 546$ GeV to be 0.215 ± 0.005 [4]. We estimate by interpolation and extrapolation the values of σ_{el}/σ_{tot} to be 0.19 ± 0.01 and 0.23 ± 0.01 at 200 and 900 GeV, respectively. Using $\sigma_{inel} = \sigma_{tot}(1-\sigma_{el}/\sigma_{tot})$ this gives for the inelastic cross section at 200 GeV, $\sigma^{200}_{inel} = 41.8 \pm 0.6$ mb, and using our measured value of R_{inel} we find $\sigma^{900}_{inel} = 50.3 \pm 0.4 \pm 1.0$ mb (first error statistical, second systematic including the error on the estimated values of σ_{el}/σ_{tot} and σ^{200}_{tot}). Using the above extrapolated value for σ_{el}/σ_{tot} we finally get

$$\sigma^{900}_{tot} = 65.3 \pm 0.7 \pm 1.5 \text{ mb}$$

Figures 9 and 10 show the energy dependence of σ_{inel} and σ_{tot}. Our deduced value of σ_{tot} at 900 GeV agrees with the dispersion relation fit of Amos et al. [3] that gives $\sigma^{900}_{tot} = 65.8$ mb.

4.2 Discussion

We compare our measurement with different fits to $\bar{p}p$ and pp total cross section data published recently. Although these fits are in good agreement with the data they rely on the only measurement available above 62 GeV, namely $\sigma_{tot} = 61.8 \pm 1.5$ mb at 546 GeV [4]. To compare predictions of σ_{tot} with our measurement of R_{inel}, we use the values of $\sigma_{el}/\sigma_{tot} = 0.23 \pm 0.01$ and 0.19 ± 0.01 at 900 and 200 GeV respectively. This implies that $R_{inel} = (0.95 \pm 0.02)R_{tot}$, where the error is due to the uncertainty in estimating σ_{el}/σ_{tot}.

One method of describing the total cross section is to use analytic forms of the scattering amplitude [15,16]. Bourrely and Martin [16] have chosen

$$F = is \frac{A + B(\ell n \frac{s}{s_o} - i\frac{\pi}{2})^2}{1 + C(\ell n \frac{s}{s_o} - i\frac{\pi}{2})^2}$$

for the even amplitude. This leads to a high energy form of the cross section (neglecting terms linear in ℓn s) like:

$$\sigma_{tot} = (A + B\ \ell n^2(s/s_o))/(1+C\ \ell n^2(s/s_o))$$

If $C = 0$, σ_{tot} saturates the Froissart bound [5] rising asymptotically like $\ell n^2 s$. However, if C is non-zero but $\ll 1$ a growth like $\ell n^2 s$ is observed in a limited energy range only, finally approaching a constant value. Bourrely and Martin [16] have considered one fit with $C = 0$ and a second fit requiring C non-zero and as large as possible whilst remaining compatible with data.

From their fit with $C = 0$ we calculate $R_{inel} = 1.264 \pm 0.025$ while from the second we find $R_{inel} = 1.208 \pm 0.024$. The quoted error is due to the interpolation we had to make to calculate the value of R. Although no definite conclusion can be made our measured value of $R = 1.20 \pm 0.01 \pm 0.02$ favours a total cross section that approaches a constant value as $s \to \infty$. A comparison of our measurement of R with the similar fits of Block and Cahn [15] again appears to favour an asymptotically constant value of σ_{tot} within this type of parametrization.

In a dispersion relation fit by Amos et al. [3] σ_{tot} is parametrized by

$$\sigma_{tot} = C_1 E^{-\nu_1} \pm C_2 E^{-\nu_2} + C_3 + C_4 \ell n^z s$$

where E is the laboratory energy, and z is determined by their fit to be 2.02 ± 0.02. The first two terms in σ_{tot} describe the low energy

behaviour, the second repesenting the difference between pp and $\bar{p}p$ cross sections, and are almost irrelevant at Collider energies. This fit yields $R_{inel} = 1.211 \pm 0.024$. The good agreement of our measured value with this fit shows that the data can be well described by a $\ell n^2 s$ rise of the total cross section.

A power law fit as suggested by Donnachie and Landshoff [23] gives $R_{inel} = 1.206 \pm 0.024$, again in agreement with our measured value. Note that this fit, although rising faster than $\ell n^2 s$, is not in contradiction with the Froissart bound assuming an asymptotic regime is still far away. In figure 11 the fits discussed above are shown in comparison with the data.

The 25% rise of the total cross section from 200 GeV to 900 GeV derived from measurement of R_{inel} and interpolation of σ_{el}/σ_{tot} is in very good agreement with a $\ell n^2 s$ growth of σ_{tot}. Together with the UA4 measurements this allows only little deviation from a $\ell n^2 s$ behaviour of the total cross section up to an energy of 1 TeV.

5. SUMMARY

The pulsed Collider worked very well making possible experiments at the highest c.m. energy reached so far. The ratio R between the $\bar{p}p$ inelastic cross sections at 900 and 200 GeV was found to be $R_{inel} = 1.20 \pm 0.01 \pm 0.02$. We deduce a total $\bar{p}p$ cross section at 900 GeV of $65.3 \pm 0.7 \pm 1.5$ mb, in agreement with a $\ell n^2 s$ increase from the ISR energy range. Our results have been compared with various published fits to the energy dependence of the $\bar{p}p$ total cross section at high energies.

ACKNOWLEDGEMENTS

The UA5 Collaboration is grateful for the tireless efforts of the SPS division staff in making the pulsed Collider a success. The physics results we have obtained at this new record energy were made possible thanks to them. We also acknowledge the excellent work of the staff of the EF division in recommissioning and running successfully the UA5 detector after a two year break from operation, and the continuing help of DD division.

We acknowledge with thanks the financial support of the Brussels group by the National Foundation for Fundamental Research and the Inter-University Institute for Nuclear Sciences, of the Bonn group by the Bundesministerium für Wissenschaft und Forschung, of the Cambridge group by the UK Science and Engineering Research Council, and of the Stockholm group by the Swedish Natural Science Research Council. Last, but not least, we acknowledge the contribution of the engineers, scanning and measuring staff of all our laboratories.

References

[1] U. Amaldi et al., Phys. Lett. 44B (1973) 112.

[2] S.R. Amendolia et al., Phys. Lett. 44B (1973) 119.

[3] N. Amos et al., Nucl. Phys. B262 (1985) 689.

[4] M. Bozzo et al., Phys. Lett. 147B (1984) 392.

[5] M. Froissart, Phys. Rev. 123 (1961) 1053.

[6] R.J. Eden, 'High Energy Collisions of Elementary Particles', Cambridge (1967) p.170.

[7] R. Castaldi and G. Sanguinetti, CERN-EP/85-36, to be published in Ann. Rev. Nucl. and Particle Science, and references therein.

[8] J. Dias de Deus, P. Kroll. J. Phys. G. 9, L81 (1983).

[9] J.Baumel, M.Feingold & M. Moshe, Nucl.Phys. B198 (1982)13.
A.R. White, Fermilab preprint CONF82/16-THY (1982).
M. Baig, J.Bartelo & J.W. Dash, Nucl.Phys B237 (1984) 502.

[10] J.G. Rushbrooke, Proc. Int. Europhysics Conference on High Energy Physics, Bari, July 1985 p.839-897.

[11] R. Henzi and P. Valin, Phys. Lett. 149B (1984) 239.

[12] J.G. Rushbrooke, CERN/EP/82-6, 18 January 1982.

[13] UA5 Collaboration, CERN/SPSC/82-75, SPSC/P184, 15 October 1982.

[14] C.M.G. Lattes et al., Phys. Rep. C65 (1980) 151.

[15] M.M. Block and R.N. Cahn, Rev. Mod. Phys. 57 (1985) 563.
M.M. Block and R.N. Cahn, Phys. Lett. 168B (1986) 151.

[16] C. Bourrely and A. Martin, CERN-TH 3931 (1984).

[17] R. Laukner, IEEE Transactions on Nuclear Science, NS-32 (1985) No.5 p.1653.

[18] UA5 Collaboration, to be submitted to Physics Reports.

[19] W. Scandale, private communication.

[20] J.G. Rushbrooke, UA5 Note, 'Experimental determination of luminosity ratio in pulsed collider operation', 22 April 1985;
R. Laukner and T. Linnecar, SPS Internal Report, 'Measurement of radial position and RF frequency at 100 GeV and 450 GeV', 30 May, 1985.
W. Middelkoop, 'Beam energies during the pulsed collider operation during March 1985', SPS Internal Report, 13 June 1985.

[21] J. Bosser et al., "Transverse emittance measurements with rapid wire scanner at CERN SPS", CERN SPS 84-11;
A. Drees, 'Bestimmung des inelastichen $p\bar{p}$ Wirkungsquerschnitts bei $\sqrt{s}$ = 900 and 200 GeV', Bonn IR 86-01.

[22] G.J. Alner et al.,'The UA5 high energy $p\bar{p}$ simulation program', to be submitted to Nucl. Inst. Meth.

[23] A. Donnachie and P.V. Landshoff, Nucl. Phys. B231 (1984) 189.

[24] V. Flaminio et al., CERN-HERA 84-01.

[25] K. Goulianos, Phys. Rep. 101 (1983) 169.

Table 1

Summary of 900 GeV Pulsed Collider Performance (Period 1 1985)

Beam energies 100 to 450 GeV

Protons per bunch (n_p)	6.10^{10}
Antiprotons per bunch ($n_{\bar{p}}$)	7.10^{9}
Emittance, protons (E_p)	$15\pi\ 10^{-6}$rad m
Emittance, antiprotons ($E_{\bar{p}}$)	$20\pi\ 10^{-6}$rad m
$\beta^*_{H,V}$	50 m
Initial luminosity at 900 GeV	$3.10^{26}cm^{-2}s^{-1}$
Bunch intensity lifetimes	4 - 6 h
Luminosity lifetime	2 - 3 h
Beam time for physics	95 h
No. of cycles (21.6s length)	16 000
Integrated luminosity at 900 GeV	6.9 μb^{-1}

Table 2

Values of trigger efficiences ε as determined from Monte Carlo simulations. Note that the errors for a given type of process (NSD or SD) are highly negatively correlated between the 1-arm and 2-arm trigger efficiencies and positively correlated between different c.m. energies. They represent an estimate of the systematic uncertainties arising from different assumptions in the models. In the SD model the main uncertainty surrounds the $\langle p_T \rangle$ of particles in the diffractively excited system; we have allowed for a range from 0.3 to 0.5 GeV. The chief uncertainty in the NSD model concerns the form of the leading particle distributions for Feynman $x > 0.95$; the quoted error corresponds to taking either a flat x-distribution or a $1-|x|$ form [25] as extreme possibilities.

$\sqrt{s}$ (GeV)	ε_1^{NSD}	ε_2^{NSD}	ε_1^{SD}	ε_2^{SD}
200	$0.067^{\mp}0.009$	0.918 ± 0.010	$0.60^{\mp}0.02$	0.06 ± 0.02
900	$0.033^{\mp}0.009$	0.950 ± 0.008	$0.48^{\mp}0.02$	0.15 ± 0.03

Table 3

Contributions to the systematic error in R.

Error source	Contribution to systematic error in R
Background correction	
1 arm sample	.7%
2 arm sample	.5%
Trigger efficiencies(*)	
NSD MC	.5%
SD MC	.4%
Luminosity ratio	1%
Total	1.5%

(*)The contributions of the trigger efficiencies to the systematic error have been derived from the values given in table 2. However, we have pessimistically ignored the likely positive correlations between different c.m. energies mentioned in table 2.

Figure Captions

Fig. 1 The 21.6 s machine cycle for the pulsed SPS Collider.

Fig. 2 The UA5 experimental layout.

Fig. 3 The relations between physical processes and different triggers.

Fig. 4 Streamer chamber photographs of a $\bar{p}p$ 2-arm trigger (a), a $\bar{p}p$ 1-arm trigger (b) and a background 1-arm trigger (c).

Fig. 5 The vertex distribution along the beam axis for 2-arm triggers (top) and 1-arm triggers (bottom). Data at 900 GeV.

Fig. 6 (a) Luminosity at 900 GeV derived from the 2-arm trigger rate. Each point represents a sample of triggers corresponding to about 500 triggers recorded on film. The points are ordered in time through several runs. (b) Ratio of corrected 2-arm cross-sections (900 GeV/200 GeV). (c) Ratio of corrected 1-arm cross-sections (900 GeV/200 GeV).

Fig. 7 The distribution of pseudorapidity gap g, defined as follows: In a SD event the rapidity of the unexcited proton is $(\ell n(\sqrt{s}/M_p)$. If η_{max} is the largest pseudorapidity of any particle observed in the event then $g = \ell n(\sqrt{s}/M_p)-\eta_{max}$. For SD events with a $1/M^2$ distribution g should be uniformly distributed, whilst NSD events in the 1-arm trigger sample tend to have g close to the minimum value allowed by the trigger.

Fig. 8 Plot of the corrected inelastic rate $\dot{N}_{900}L_{200}/L_{900}$ against $\dot{N}_{200}$. Each point corresponds to a ~ 500 picture run, as in fig 6. The line corresponds to $R_{inel} = 1.20$.

Fig. 9 The inelastic pp and $\bar{p}p$ cross-sections as a function of the c.m. energy $\sqrt{s}$. Data from refs [3,4,24].

Fig. 10 The total cross-section for pp and $\bar{p}p$ as a function of the c.m. energy $\sqrt{s}$. Data from refs [3,4,24].

Fig. 11 As fig 10 with various fits superimposed.

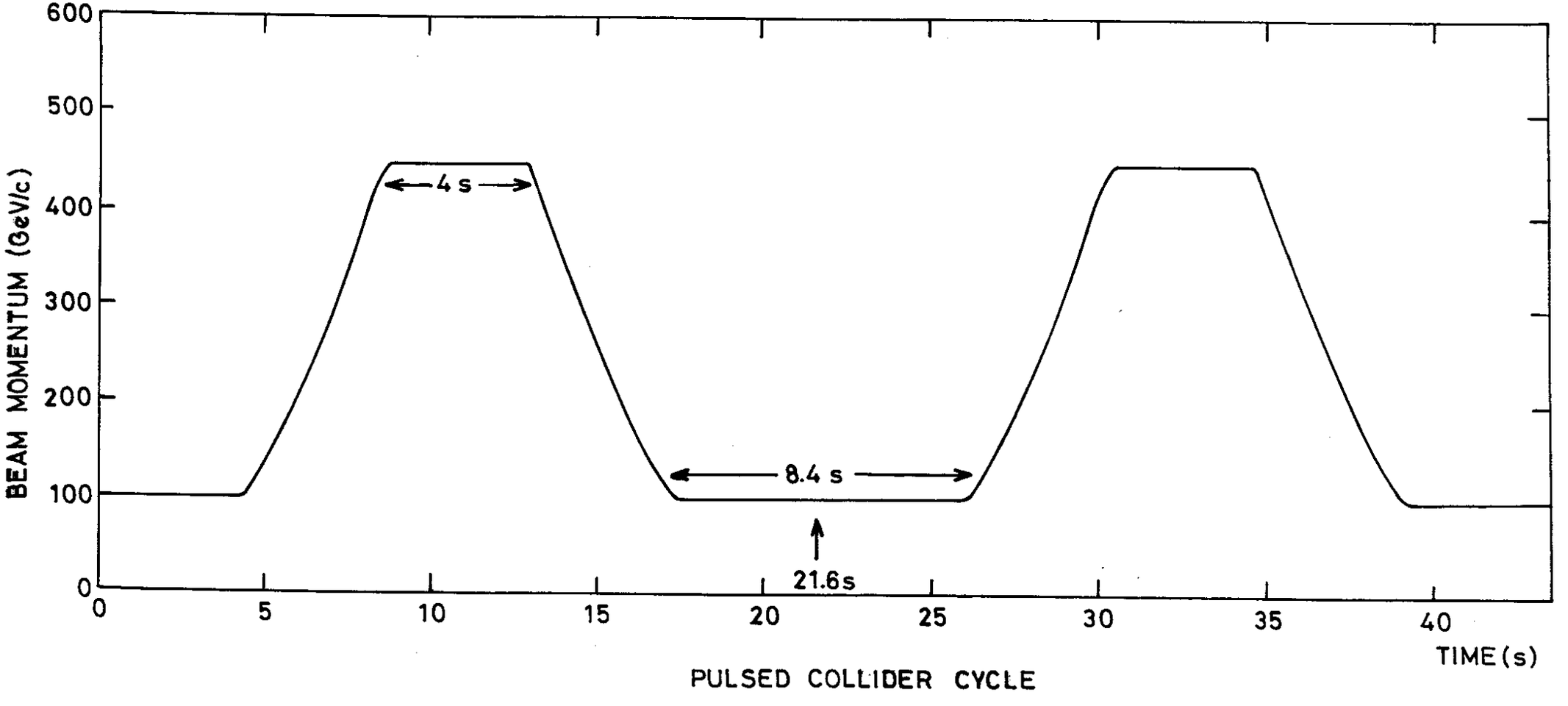
600
500
400
300
200
100
0
BEAM MOMENTUM (GeV/c)
4 s
8.4 s
21.6s
0
5
10
15
20
25
30
35
40
TIME (s)
PULSED COLLIDER CYCLE

FIG. 1

SCHEMATIC LAYOUT OF THE STREAMER CHAMBER SYSTEM

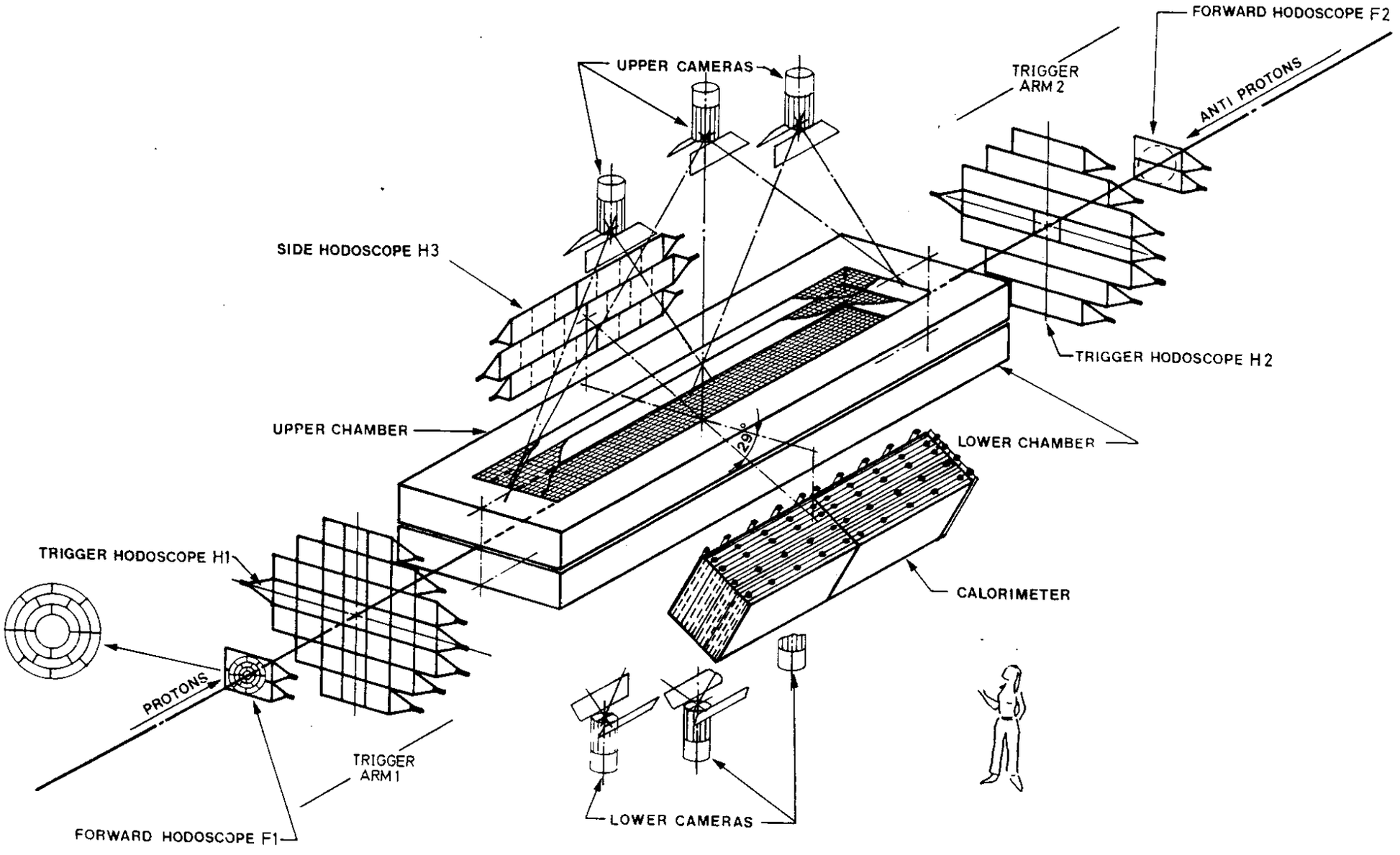

FIG.2

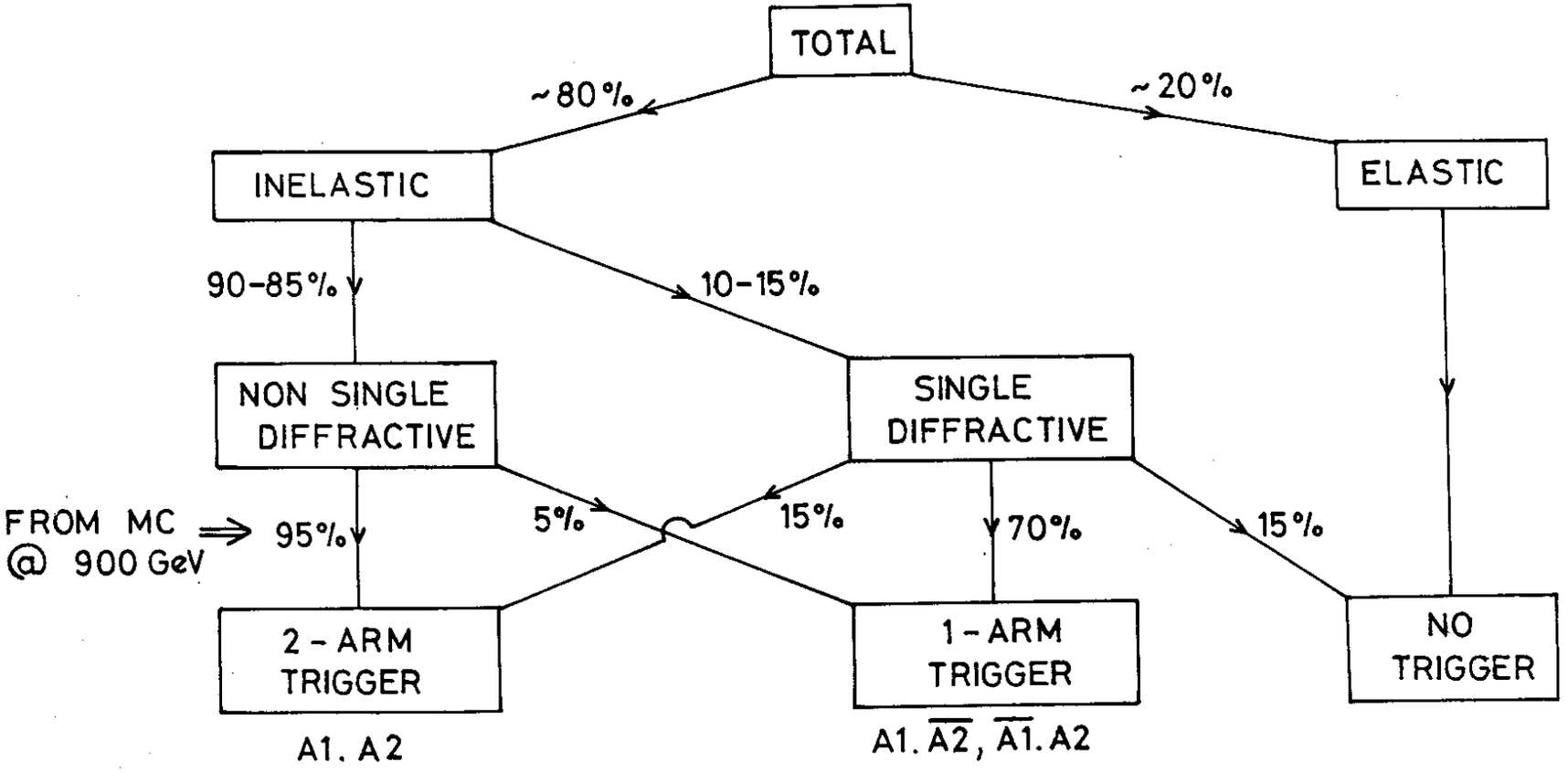
TOTAL
~80%
~20%
INELASTIC
ELASTIC
90-85%
10-15%
NON SINGLE DIFFRACTIVE
SINGLE DIFFRACTIVE
FROM MC @ 900 GeV
95%
5%
15%
70%
15%
2 - ARM TRIGGER
1 - ARM TRIGGER
NO TRIGGER
A1. A2
A1. $\overline{A2}$, $\overline{A1}$. A2

FIG. 3

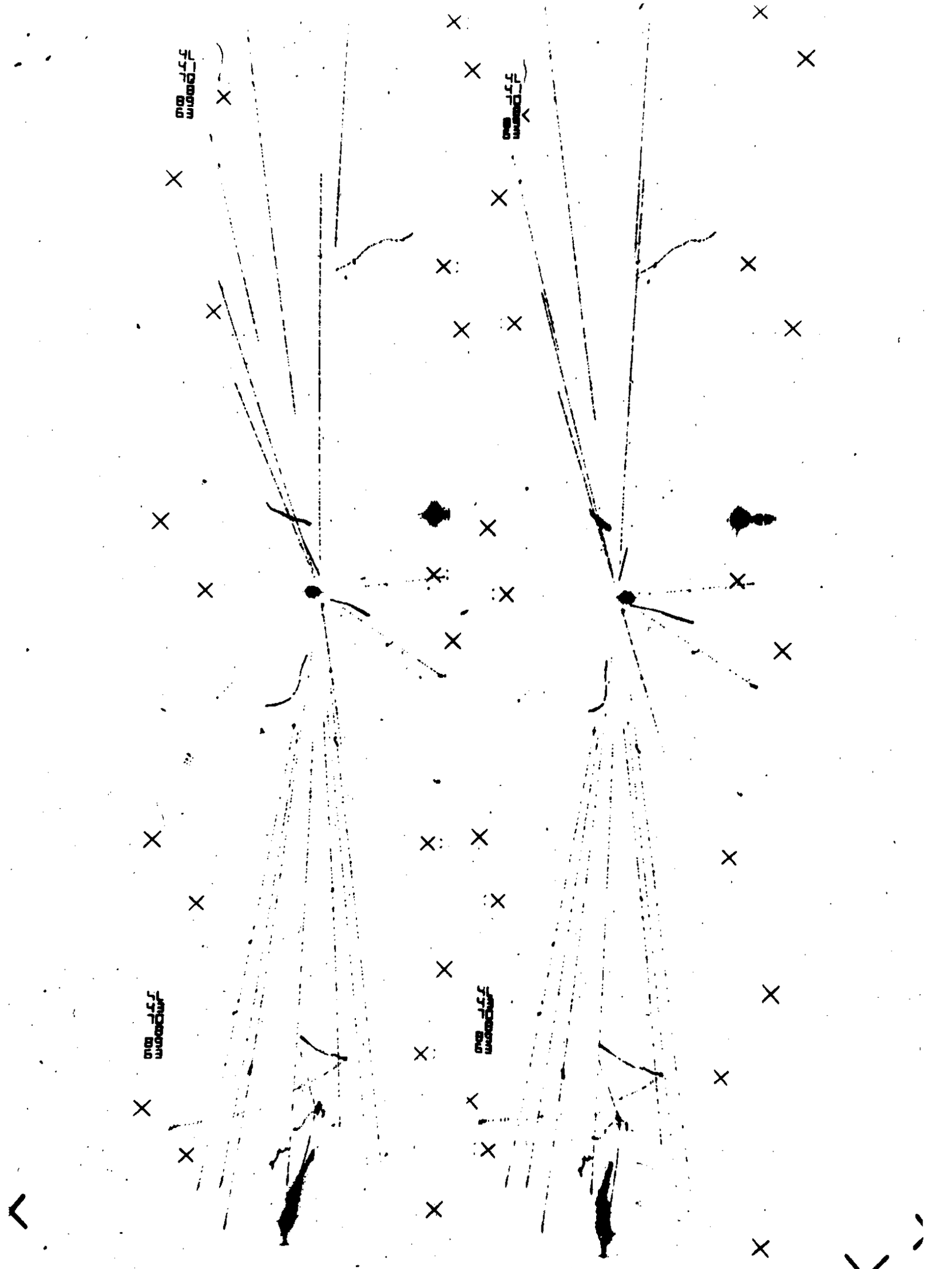

FIG.4(A)

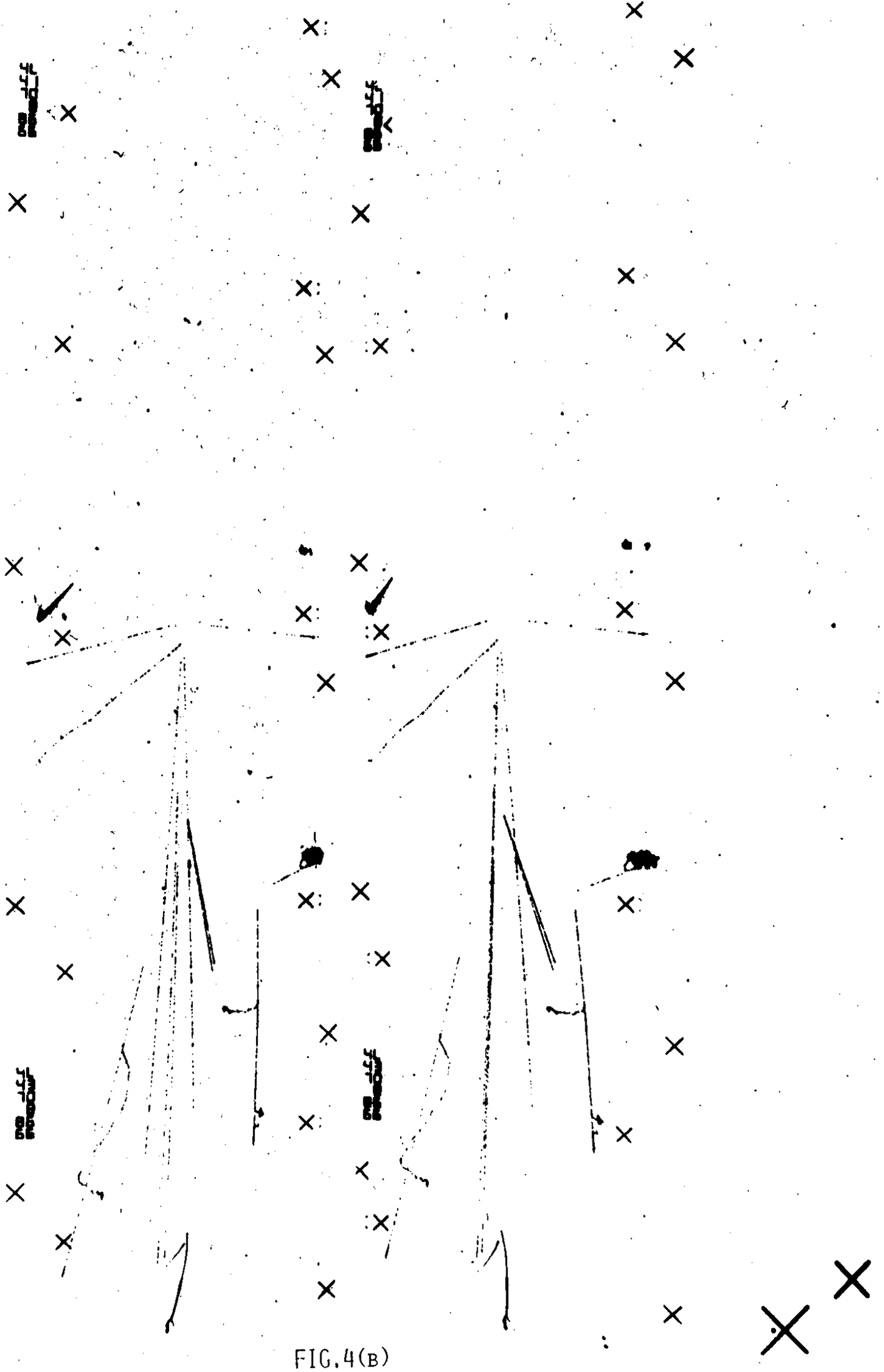

FIG.4(B)

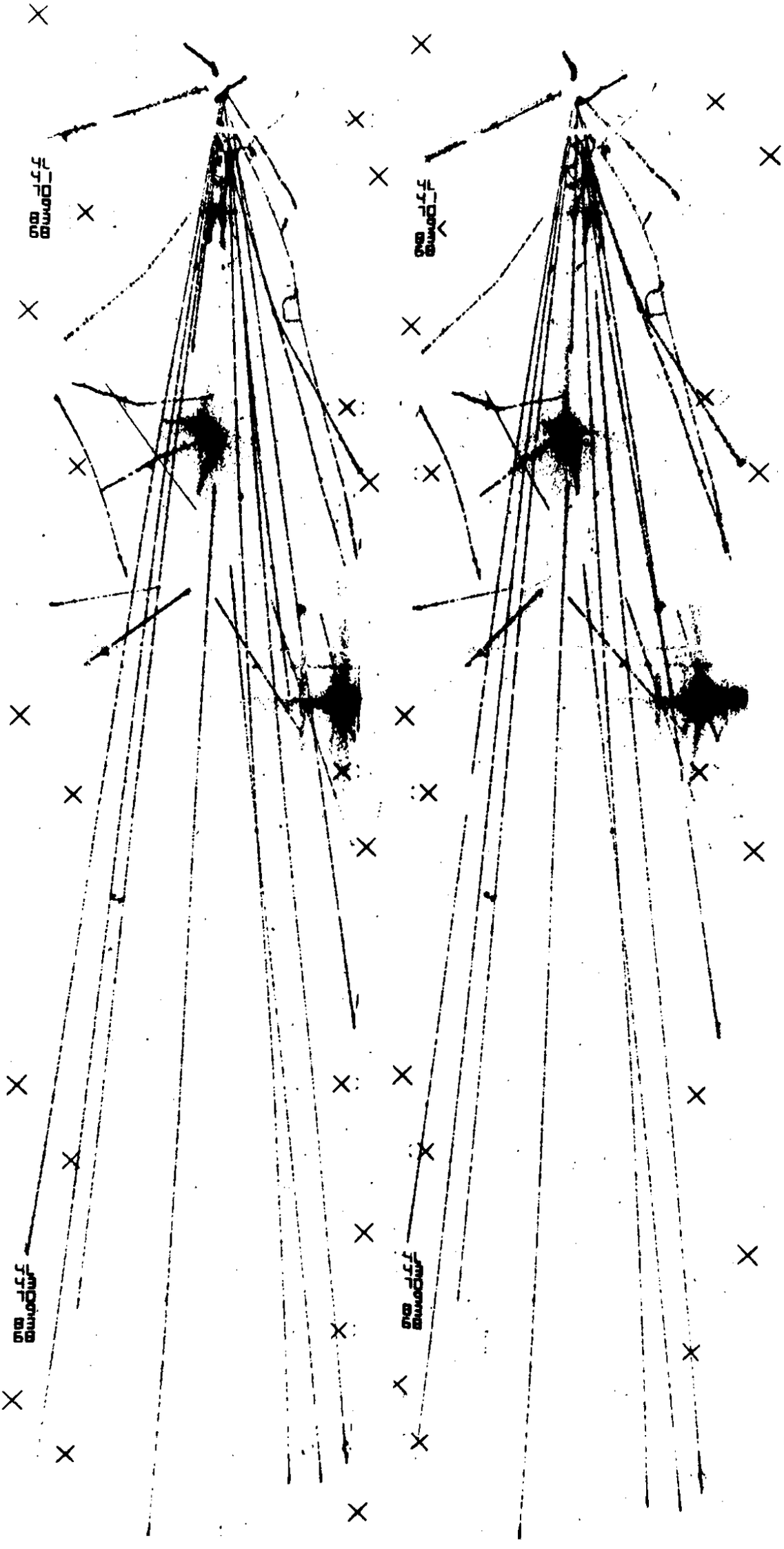

FIG.4(c)

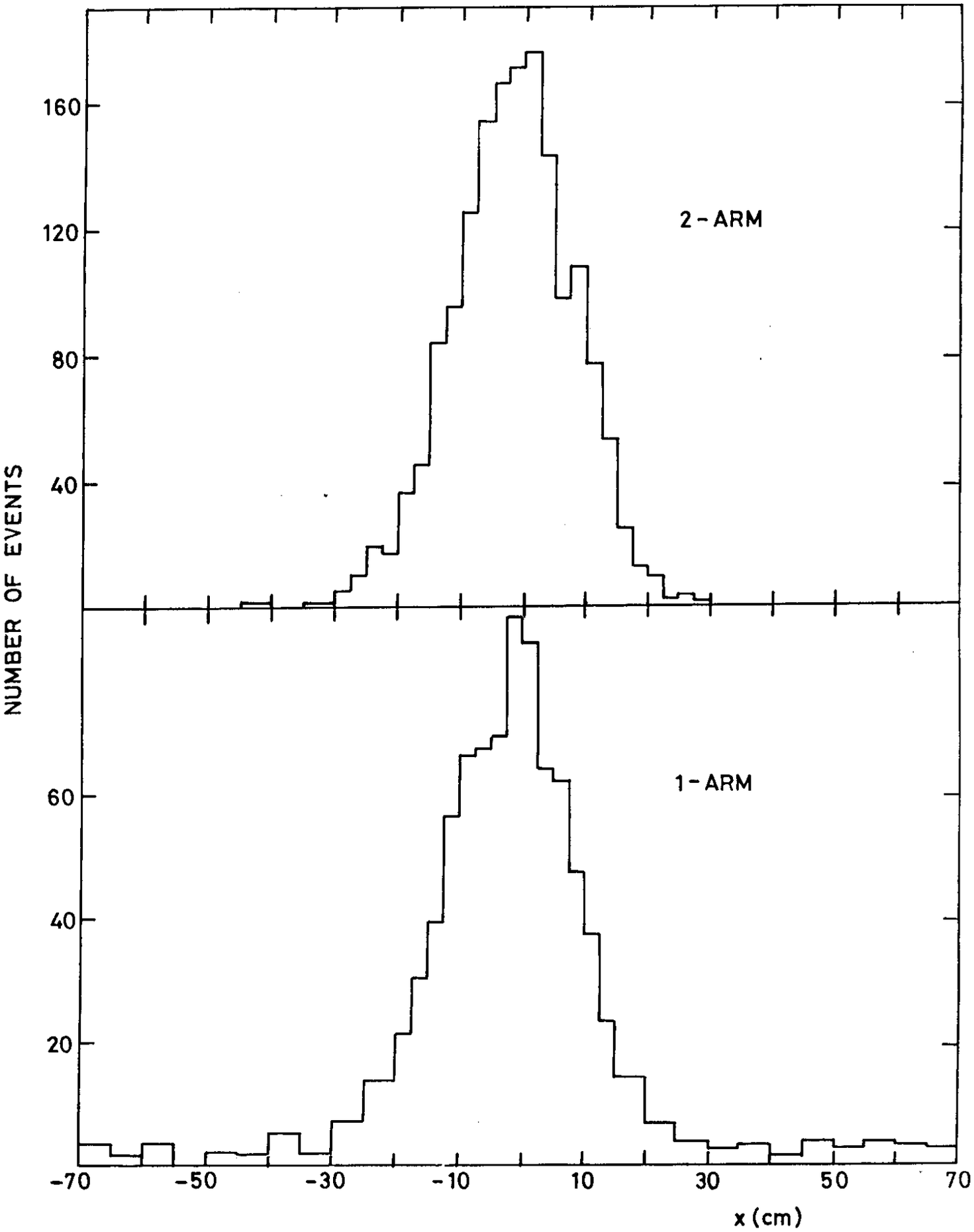
NUMBER OF EVENTS
160
120
80
40
2 - ARM
60
40
20
1 - ARM
-70
-50
-30
-10
10
30
50
70
x (cm)

FIG. 5

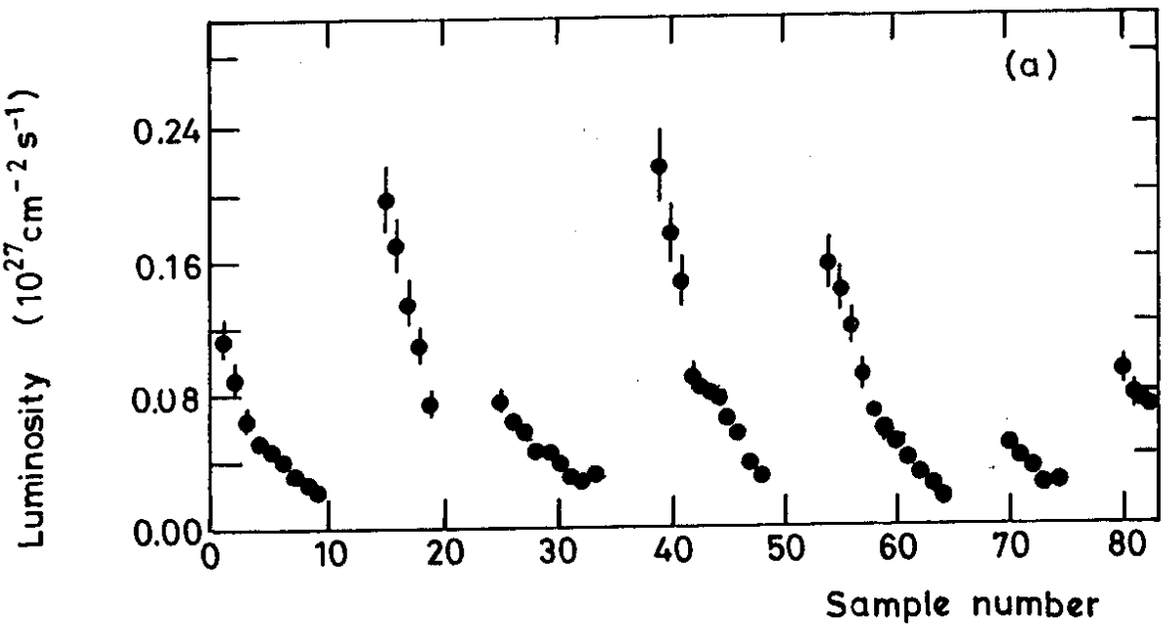
(a)
Luminosity (10^{27}cm^{-2}s^{-1})
0.24
0.16
0.08
0.00
0
10
20
30
40
50
60
70
80
Sample number

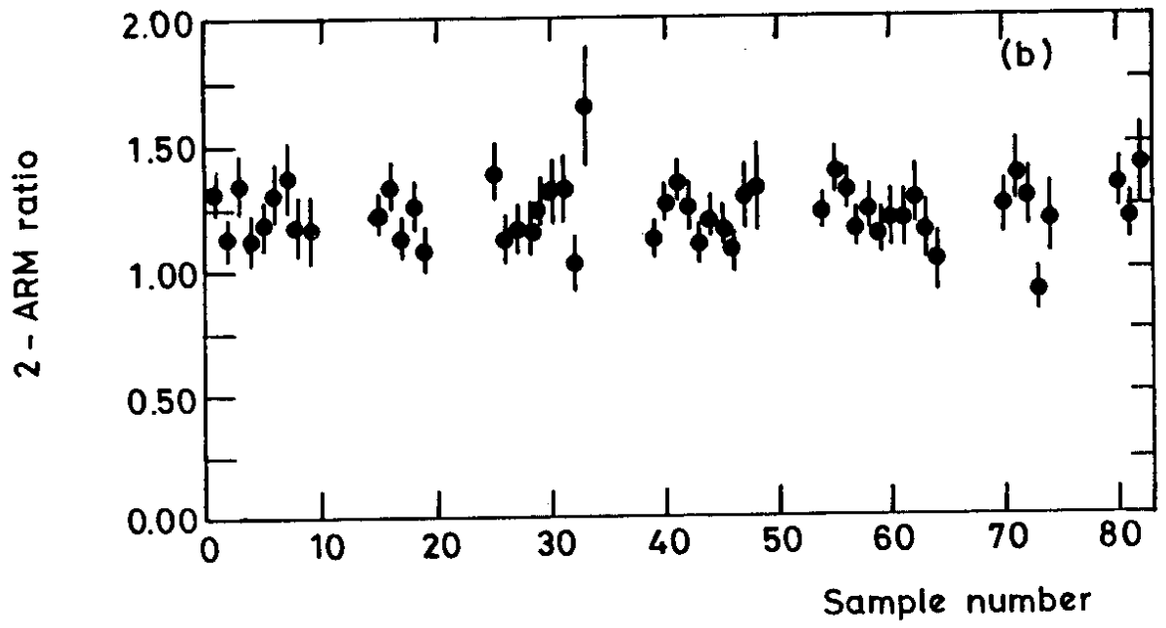
(b)
2 - ARM ratio
2.00
1.50
1.00
0.50
0.00
0
10
20
30
40
50
60
70
80
Sample number

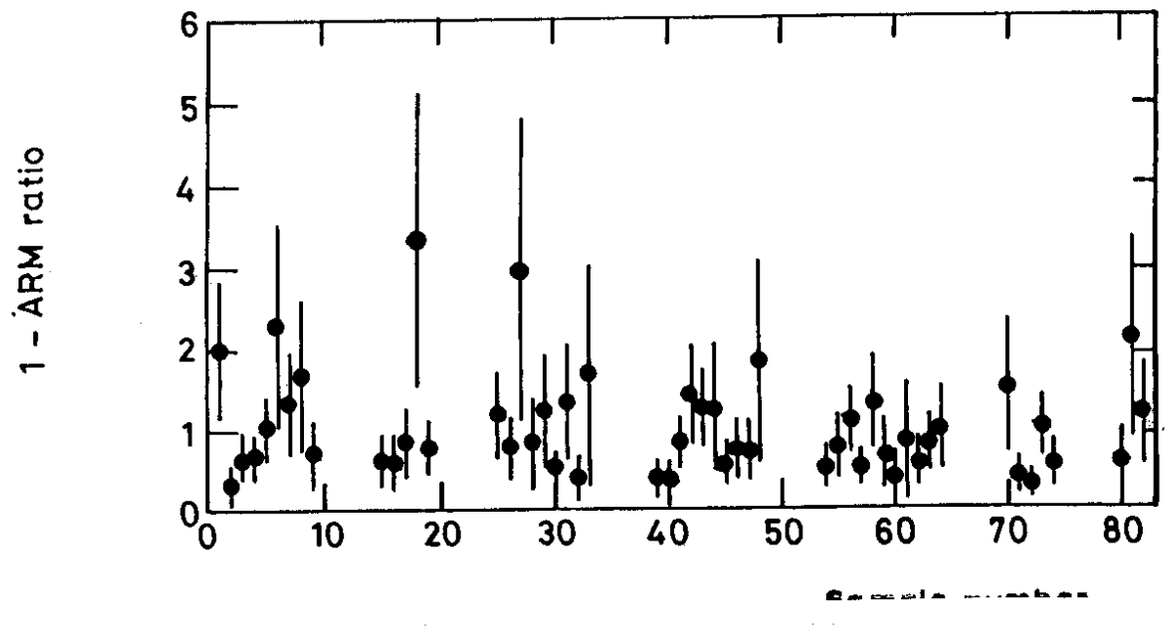
1 - ARM ratio
6
5
4
3
2
1
0
0
10
20
30
40
50
60
70
80

Fig. 6

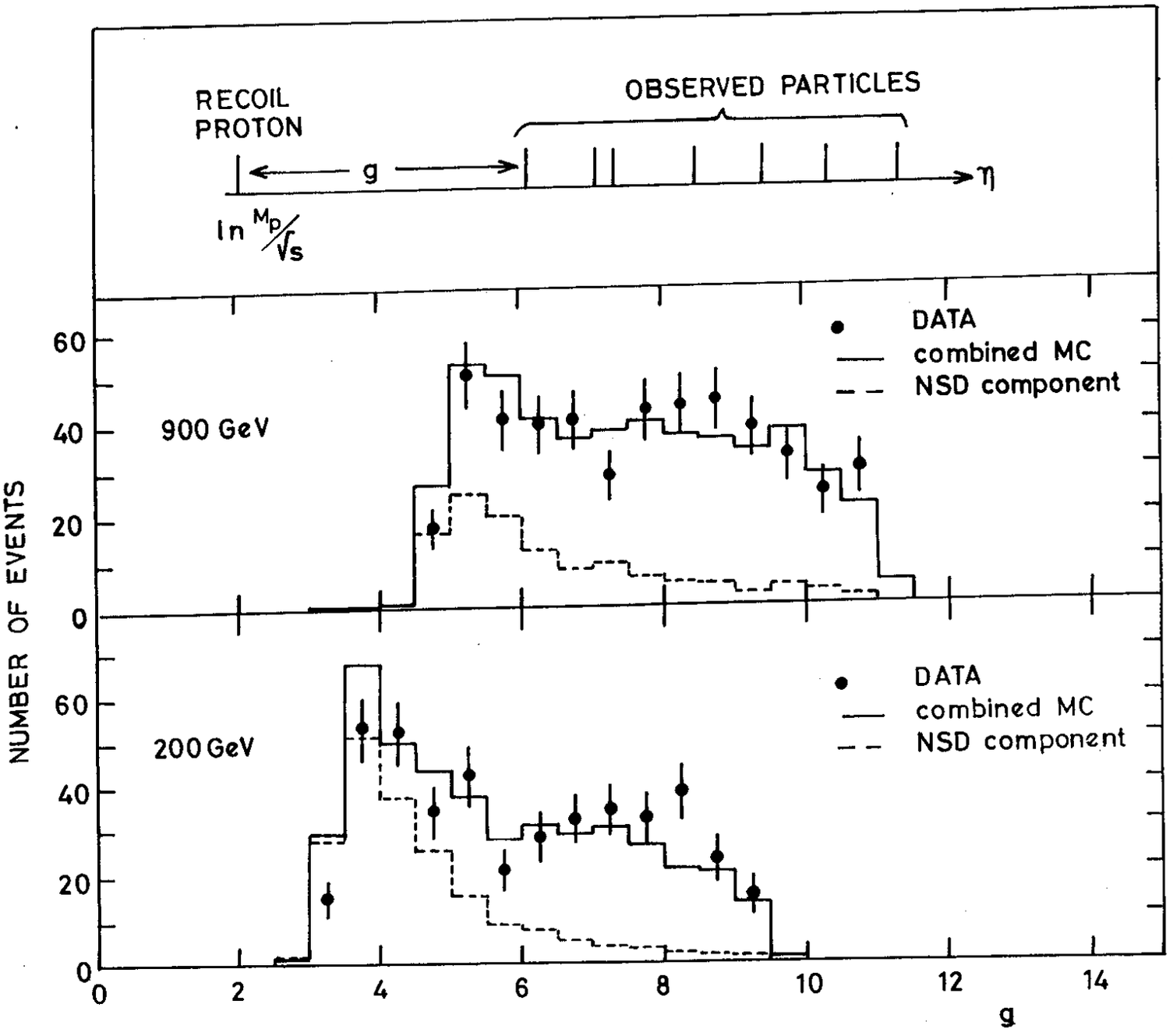
RECOIL
PROTON
OBSERVED PARTICLES
g
η
ln Mp/√s
DATA
combined MC
NSD component
900 GeV
200 GeV
NUMBER OF EVENTS
0
20
40
60
0
2
4
6
8
10
12
14
g

FIG. 7

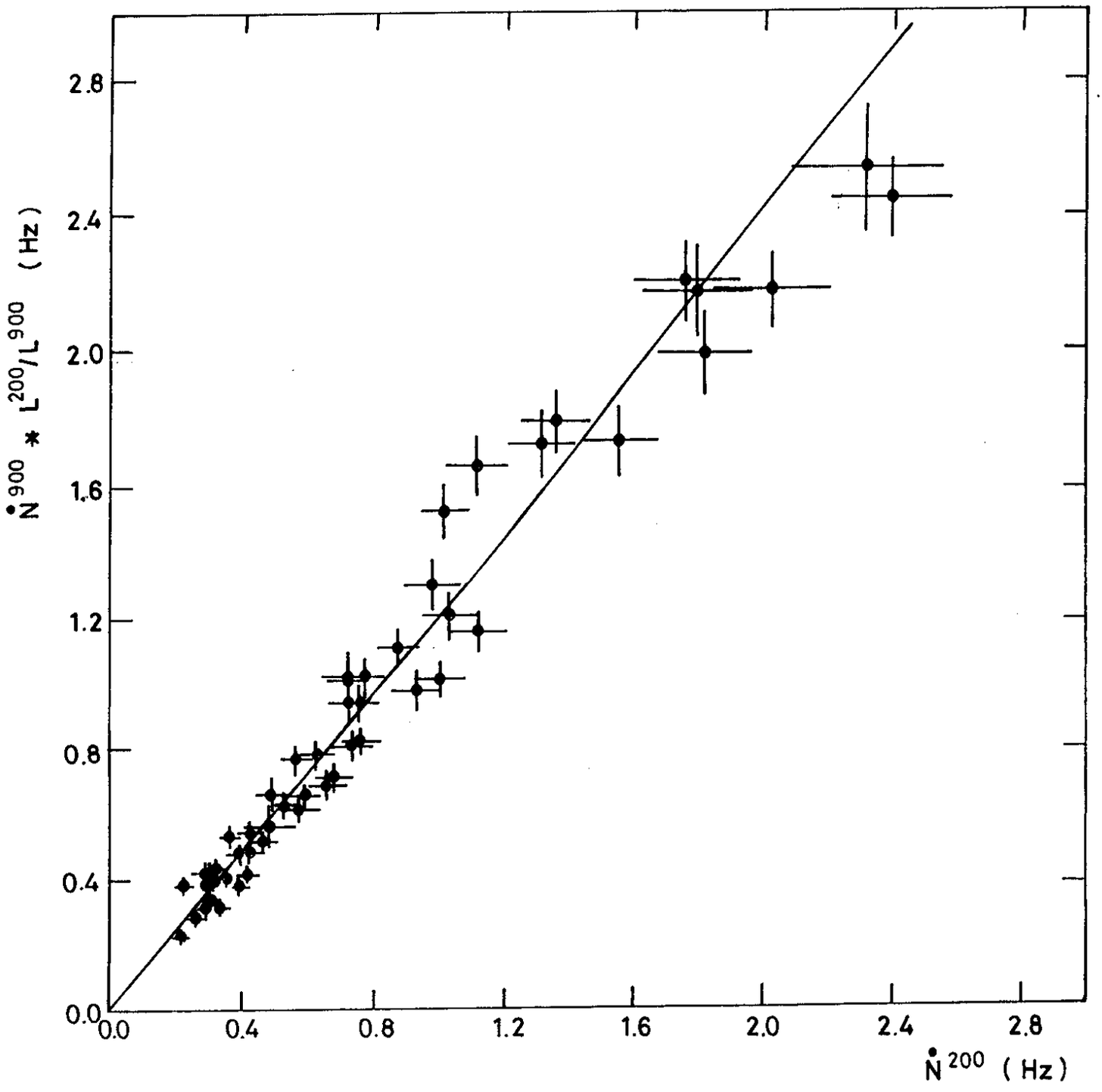
2.8
2.4
2.0
1.6
1.2
0.8
0.4
0.0
0.0
0.4
0.8
1.2
1.6
2.0
2.4
2.8
$\dot{N}^{900} * L^{200}/L^{900}$ (Hz)
$\dot{N}^{200}$ (Hz)

FIG.8

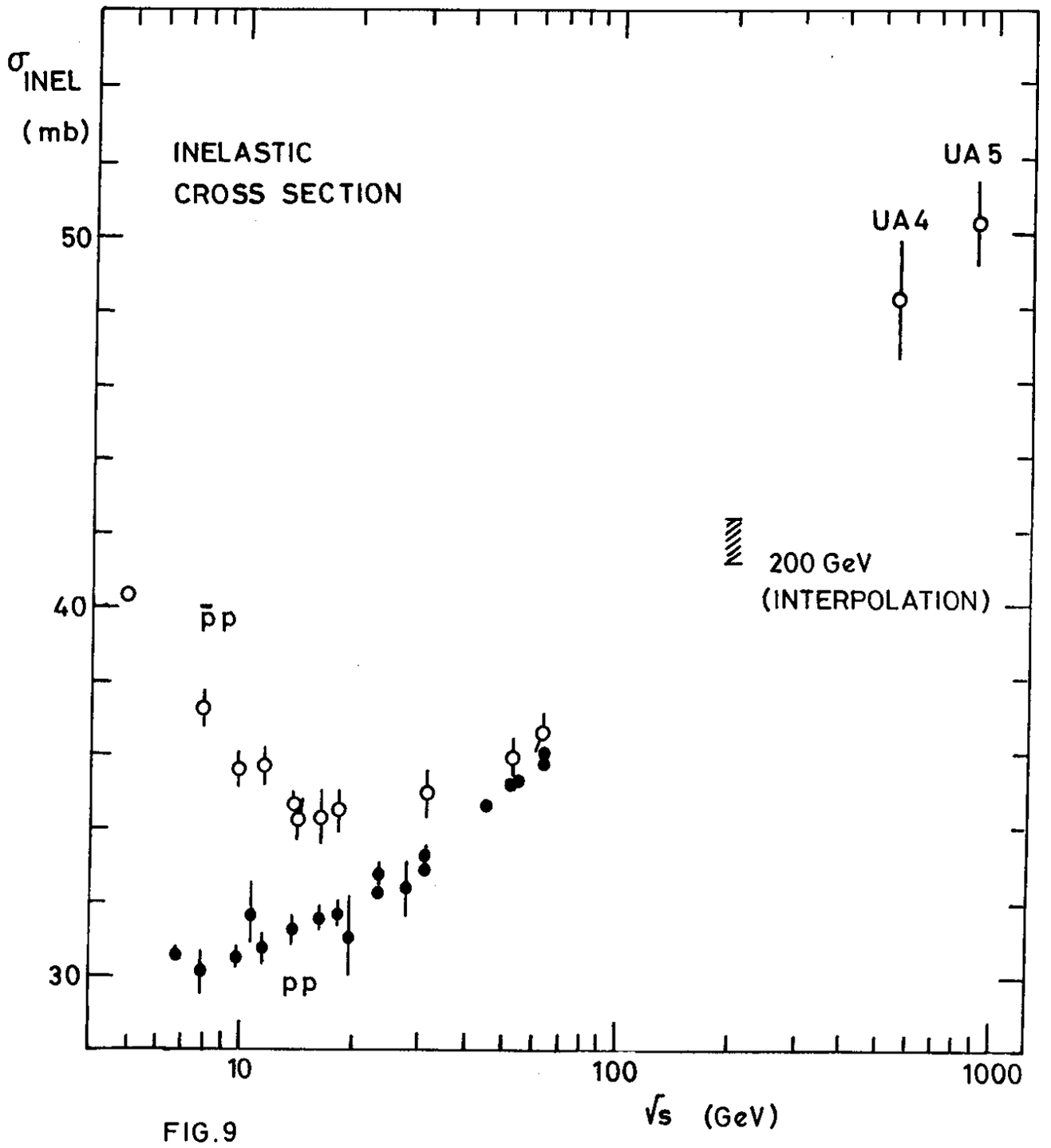
σ INEL
(mb)
INELASTIC
CROSS SECTION
UA 5
UA 4
50
40
30
200 GeV
(INTERPOLATION)
p̄p
pp
10
100
1000
√s (GeV)

FIG.9

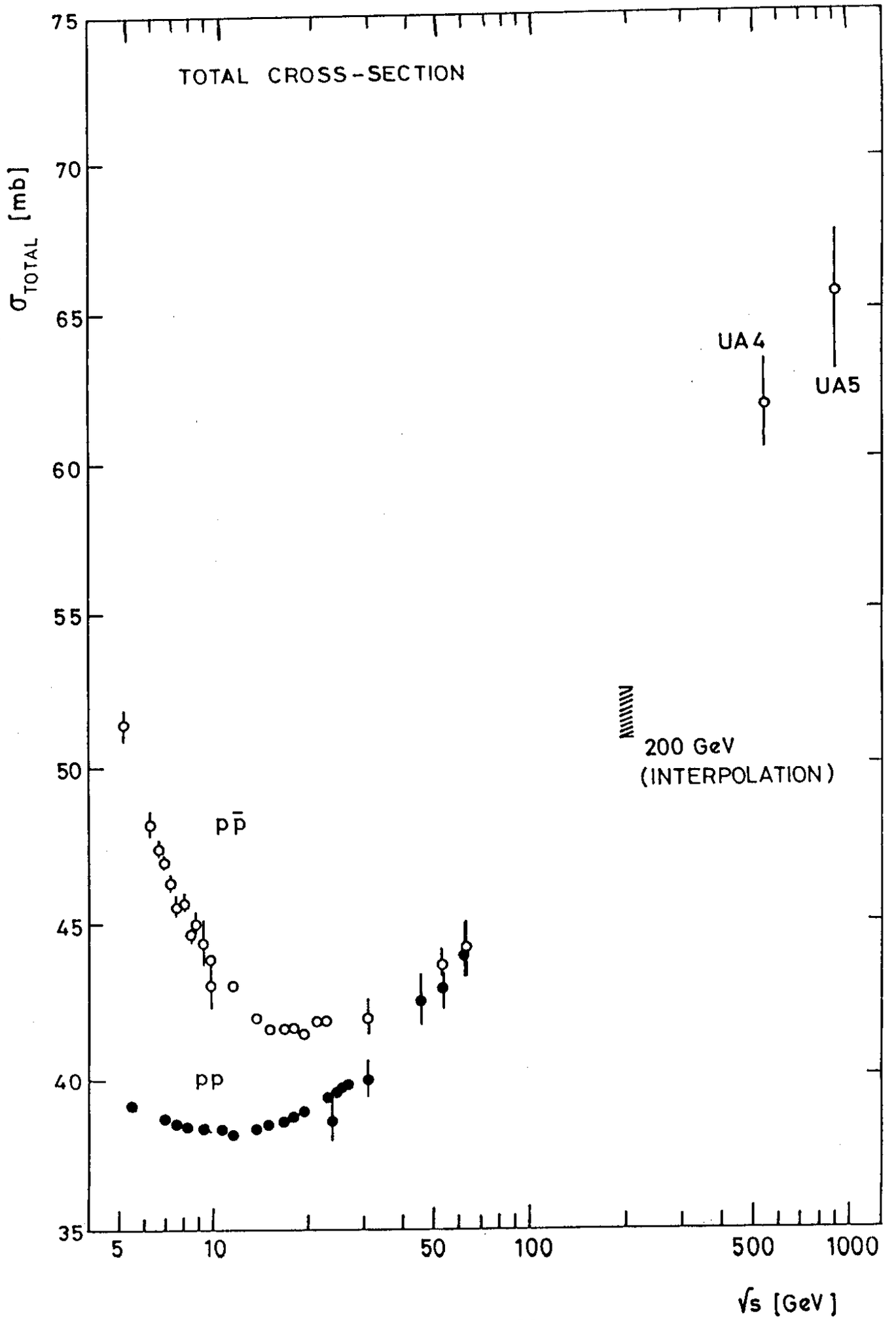
TOTAL CROSS-SECTION
σ_{TOTAL} [mb]
75
70
65
60
55
50
45
40
35
5
10
50
100
500
1000
$\sqrt{s}$ [GeV]
UA4
UA5
200 GeV
(INTERPOLATION)
$p\bar{p}$
pp

Fig. 10

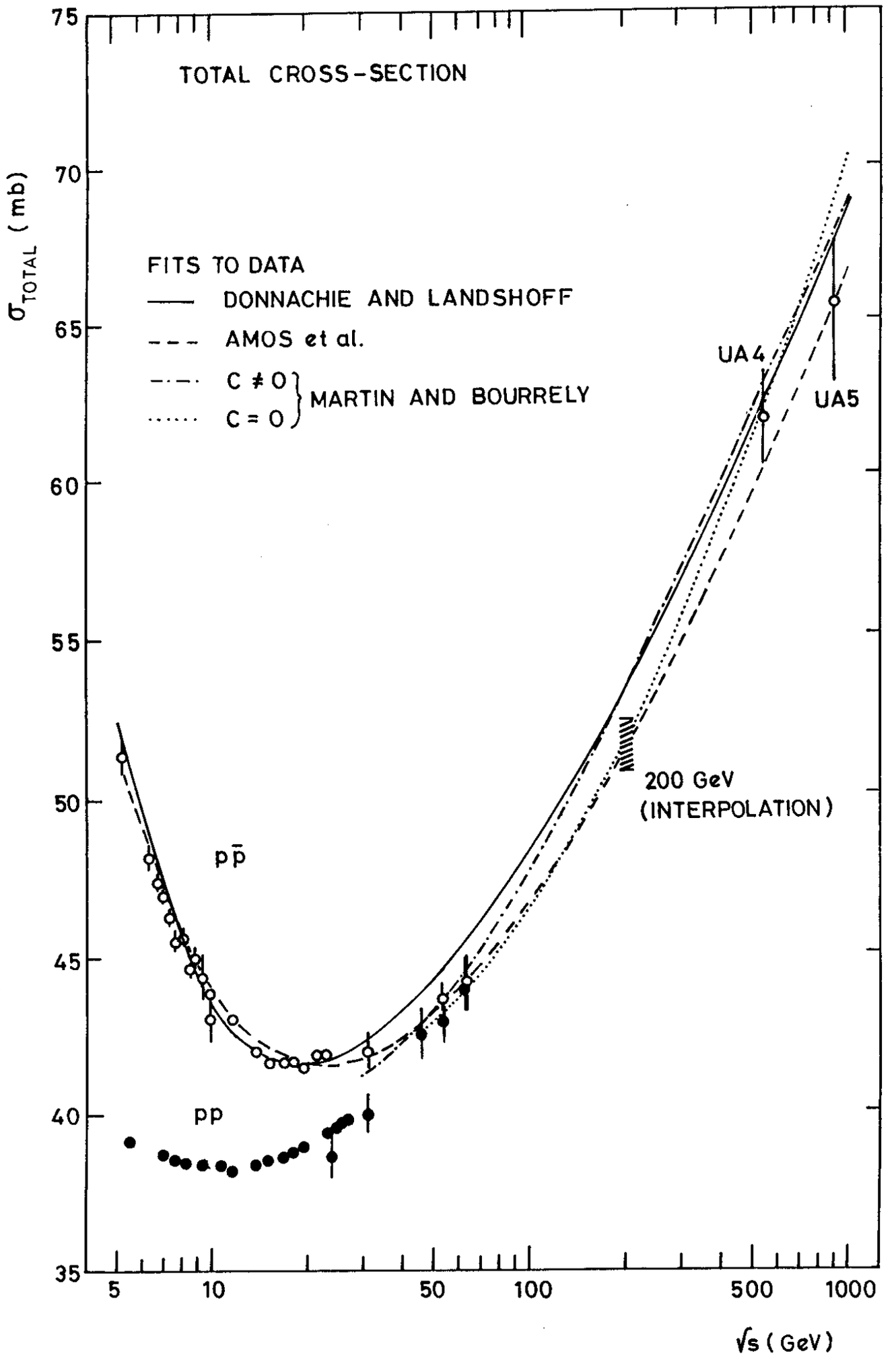
TOTAL CROSS-SECTION
σ_{TOTAL} (mb)
FITS TO DATA
DONNACHIE AND LANDSHOFF
AMOS et al.
C ≠ 0
C = 0
MARTIN AND BOURRELY
UA4
UA5
200 GeV
(INTERPOLATION)
$p\bar{p}$
pp
75
70
65
60
55
50
45
40
35
5
10
50
100
500
1000
$\sqrt{s}$ (GeV)

FIG. 11